NEUTRON FORM FACTORS FROM ELASTIC ELECTRON-DEUTERON SCATTERING

Thomas Walter Mader

United States
Naval Postgraduate School

THESIS

NEUTRON FORM FACTORS FROM
ELASTIC ELECTRON-DEUTERON SCATTERING

by

Thomas Walter Mader

Thesis Advisor: F. R. Buskirk

June 1971

Approved for public release; distribution unlimited.

Neutron Form Factors from Elastic Electron-Deuteron Scattering

by

Thomas Walter Mader
Ensign, United States Navy
A.B., University of California, Berkeley, 1970

Submitted in partial fulfillment of the
requirements for the degree of

MASTER OF SCIENCE IN PHYSICS

from the

NAVAL POSTGRADUATE SCHOOL
June 1971

ABSTRACT

Utilizing a gas target in electron-deuteron and electron-proton scattering, measurements of the ratio of the deuteron to proton form factor, G_{ed}/G_{ep}, were made within a precision of 0.8 to 1.3 percent for the range of momentum transfers, q^2, from 0.05 to 0.60 inverse Fermis squared and for scattering angles between 60 and 120 degrees. From G_{ed}/G_{ep} the neutron to proton form factor ratio, G_{en}/G_{ep}, was extracted utilizing the deuteron structure factor, as calculated from the Feshbach-Loman wave functions, and relativistic corrections. The values of G_{en}/G_{ep} found failed to support previous measurements which agreed with the thermal neutron-electron interaction slope.

TABLE OF CONTENTS

I. INTRODUCTION ---------- 7

II. DETERMINATION OF THE NEUTRON CHARGE FORM FACTOR- 10

III. DATA REDUCTION ---------- 15

A. THE RATIO EXPERIMENT ---------- 15

B. ANALYSIS OF SCATTERING PEAKS ---------- 22

IV. RESULTS ---------- 29

LIST OF REFERENCES ---------- 36

INITIAL DISTRIBUTION LIST ---------- 37

FORM DD 1473 ---------- 38

LIST OF TABLES

TABLE

I. Comparison of Radiative Correction Calculations -- 21

II. A Summary of Calculations for G^2_{ed}/G^2_{ep} ---------- 31

III. Least Squares Fits for G_{ed}/G_{ep} ---------- 32

IV. A Summary of Calculations for $G_{en} + \Delta G_{en}$ --------- 34

LIST OF FIGURES

FIGURE

1. Hydrogen Elastic Peak at 0.1534 F^{-2} ---------- 25

2. Mixture Experiment at 0.3618 F^{-2} ---------- 26

3. Deuterium Experiment at 0.3618 F^{-2} with Elastic and Inelastic Peaks ---------- 27

4. Mixture Experiment at 0.1610 F^{-2} ---------- 28

5. G_{ed}/G_{ep} versus q^2 ---------- 33

6. $G_{en} + \Delta G_{en}$ versus q^2 ---------- 35

ACKNOWLEDGEMENT

The author wishes to express his sincere graditude for the advice and assistance received from his thesis advisor, Professor F. R. Buskirk.

I. INTRODUCTION

The term, "neutron-electron (n-e) interaction," is used to describe part of the electromagnetic interaction between the neutron and the electron. The neutron has zero total charge and therefore there is no Coulomb interaction between a neutron and an electron. However, both particles have magnetic moments resulting in a spin-dependent magnetic dipole-dipole interaction. Furthermore, there is a velocity dependent interaction between the magnetic moment of the neutron and the magnetic field associated with the electron convection current. These interactions have been well documented and are not of interest here [6]. If there is a non-zero charge distribution with the neutron, (i.e., a charge separation) then any charged particle probing the neutron will experience spin and velocity independent electrostatic forces. These are the forces of interest in the n-e interaction.

Since a free neutron has an anomalous magnetic moment, some charge separation in the neutron can be expected. This contribution to the interaction is called the magnetic or Foldy term [5]. The remaining interaction (due to charge separation) is a result of the fact that a neutron can dissociate into a negative pion and a porton.

$$n \longleftrightarrow p + \pi^-$$

If the neutron spends part of the time as a proton and negative pion, say 20%, then the electron penetrating the neutron

would "see" an electric field equal to that produced by a charge of 0.2e, e being the proton charge. The force of this positive charge would be attractive and of short range due to screening effects of the negative pion.

The most accurate measurements of the n-e interaction have been by Krohn and Ringo [7] (1966) utilizing a technique of Fermi and Marshall [3] (1947). The Krohn and Ringo determinations yield the slope of the neutron charge form factor at low momentum transfers as

$$dG_{en}/d(q^2) = 0.0193 \text{ + or - } 0.0004.$$

From experiments done at the High Energy Physics Laboratory, Stanford University and at the Naval Postgraduate School LINAC, J. Stewart was able to show that the Feshbach-Loman wave functions together with relativistic corrections remove previous discrepancies between the neutron electron slope at $q^2 = 0$ and the slope given by values of G_{en} obtained in electron scattering in the range of momentum transfers from 0.10 to 0.80 inverse Fermis squared [8]. Stewart's measurements utilized a solid deuterized polyethylene $(CD_2)_n$ target for the electron-deuteron interaction and a solid polyethylene $(CH_2)_n$ target for the electron-proton interaction. These experiments yielded a n-e interaction slope of

$$dG_{en}/d(q^2) = 0.0179 \text{ + or - } 0.0036.$$

The experiments utilizing polyethylene targets have the disadvantage of requiring a subtraction of the carbon scattering from proton or deuteron scattering. If a pure gas target is used, proton or deuteron data can be obtained directly. In these measurements a cylindrical target cell contained deuterium or hydrogen gas at pressures of approximately 150 PSI and temperatures in the liquid nitrogen range. The target cell "windows" were made of thin (0.001 inch) stainless steel which does cause a beam energy loss, but does not give an observed elastic peak like the carbon in the polyethylene targets. The high pressure and low temperature conditions of the gas increase the target density nearly forty times over that at standard temperature and pressure. An accurate ratio of the hydrogen to deuterium gas densities can be obtained from pressure readings, if the temperature is held constant.

II. DETERMINATION OF THE NEUTRON CHARGE FORM FACTOR

The theoretical cross section (Mott cross section) for a point nucleon is expressed by

$$\left(\frac{d\sigma}{d\Omega}\right)_{Mott} = \left(\frac{e^2}{2E_i}\right)^2 \frac{\cos^2 \theta/2}{\sin^4 \theta/2} \frac{1}{\xi} \qquad (2\text{-}1)$$

where

$$\xi = 1 + \frac{2E_i}{M} \sin^2 \theta/2 \qquad (2\text{-}2)$$

is the recoil factor. The ratio of the experimental cross section to the prediction for a point nucleon will yield the square of the total form factor G^2. For a proton

$$G_p^2 = \frac{(G_{ep}^2 + \tau G_{mp}^2)}{1 + \tau} + 2\tau \tan^2 \theta/2 \; G_{mp}^2 \qquad (2\text{-}3)$$

where G_{ep} and G_{mp} are the charge and magnetic form factors respectively. Equation (2-3) may be written

$$G_p^2 = \frac{G_{ep}^2}{1 + \tau} + \frac{\tau G_{mp}^2}{1 + \tau} [1 + 2(1+\tau)\tan^2 \theta/2] \qquad (2\text{-}4)$$

where $\tau = - q^2/M_p^2$ and $q^2 = \vec{q}^2 - q_o^2$. Therefore, within the range of momentum transfers considered, τ^2 terms may be neglected. Furthermore, utilizing the scaling law, $G_{mp} = \mu_p G_{ep}$ Equation (2-4) reduces to

$$G_p^2 = \frac{G_{ep}^2}{1 + \tau} [1 + \tau\mu_p^2(1 + 2\tan^2 \theta/2)]. \qquad (2\text{-}5)$$

An expression for G_{ep}, the proton charge form factor, is then obtained.

$$G_{ep}^2 = \frac{G_p^2 \ (1 + \tau)}{(\ 1 + C_p)} \qquad (2\text{-}6)$$

where

$$C_p = \tau\mu_p^2(1 + 2\tan^2\ \theta/2). \qquad (2\text{-}7)$$

$K_M^p = (1 + \tau)/(1 + C_p)$ can be considered the magnetic correction term applied to the total form factor, G_p^2, to obtain the charge form factor G_{ep}^2.

For the deuteron

$$G_d^2 = G_e^2 + \frac{8}{9}\eta^2 G_Q^2 \ + \frac{2}{3}\eta G_m^2 \ [1 + 2(1-\eta)\tan^2\ \theta/2] \qquad (2\text{-}8)$$

where G_e is the charge form factor, G_Q is the quadrupole form factor, and G_m is the magnetic form factor. $\eta = -\ q^2/M_d^2$, and therefore, the $1 - \eta$ term approaches 1 within the range of momentum transfers considered. Expressions for the form factors (including static limits) are

$$G_e = (G_{ep} + G_{en})\ D_c \xrightarrow[q^2=0]{} 1 \qquad (2\text{-}9)$$

and

$$G_Q = (G_{ep} + G_{en})\ D_Q \xrightarrow[q^2=0]{} M_d^2 Q \qquad (2\text{-}10)$$

and

$$G_m = (G_{ep} + G_{en})\ D_m^e + (G_{mp} + G_{mn})\ D_m^m \xrightarrow[q^2=0]{} \frac{M_d}{M_p}\ \mu_d \qquad (2\text{-}11)$$

where D_c is the charge structure factor, D_Q is the quadrupole moment structure factor, D_m^m accounts for the contribution of the intrinsic magnetic moments of the proton and neutron to the scattering process, and D_m^e is the magnetic contribution to the scattering process arising from the convection of

charge in the deuteron [8]. Equation (2-11) may be simplified utilizing the scaling laws,

$$G_{md} = \mu_d' G_{ed} \quad , \quad \mu_d' = \frac{M_d}{M_p} \mu_d$$

and

$$\frac{G_{mp}}{\mu_p} = \frac{G_{mn}}{\mu_n} = G_{ep}.$$

Hence,

$$G_m = (G_{ep} + G_{en})\mu_d' D_c. \tag{2-12}$$

Therefore the total form factor is given by

$$G_d^2 = (G_{ep}+G_{en})^2\{D_c[1+\tfrac{2}{3}\eta\mu_d'^2(1+2\tan^2 \theta/2)]+\tfrac{8}{9}\eta^2 D_Q^2\}. \tag{2-13}$$

Due to the size of η in the range of momentum transfers considered, the quadrupole term can be neglected giving rise only to minor corrections. In a manner analogous to the proton case, the deuteron charge form factor is given by

$$G_{ed}^2 = (G_{ep} + G_{en})^2 D_c^2 = \frac{G_d^2}{1 + C_d} \tag{2-14}$$

where

$$C_d = \tfrac{2}{3}\eta\mu_d'^2(1 + 2\tan^2 \theta/2). \tag{2-15}$$

$K_M^p = 1/(1 + C_d)$ can be considered the magnetic correction term applied to the total form factor, G_d^2, to obtain the charge form factor, G_{ed}^2.

Define F_d', the deuteron structure factor.

$$F_d' = D_c^2[1+\tfrac{2}{3}\eta\mu_d'^2(1+2\tan^2 \theta/2)]+\tfrac{8}{9}\eta^2 D_Q^2. \tag{2-16}$$

Therefore, Equation (2-13) simplifies to

$$G_{ed}^2 = (G_{ep} + G_{en})^2 F_d^2 \qquad (2\text{-}17)$$

where $F_d^2 = (1 + C_d)F_d'^2$. Hence, the neutron charge form factor, G_{en}, is given in the following terms

$$G_{en} = \frac{1}{F_d} G_{ed} - G_{ep}. \qquad (2\text{-}18)$$

There is still the task of finding F_d. Notice from Equation (2-16) that D_c, the charge structure factor, and D_Q, the quadrupole moment structure factor, are needed. These are given by

$$D_c(\vec{q}) = \int_0^\infty [u^2(r) + w^2(r)] j_0\left(\frac{|\vec{q}|r}{2}\right) dr \qquad (2\text{-}19)$$

$$D_Q(\vec{q}) = \frac{6\sqrt{2}}{q^2} M_d^2 \int_0^\infty [u(r)w(r) - \frac{w^2(r)}{\sqrt{8}}] j_2\left(\frac{|\vec{q}|r}{2}\right) dr \qquad (2\text{-}20)$$

where j_0 and j_2 are spherical Bessel functions. $u(r)$ and $w(r)$ are appropriate deuteron wave functions. Feshbach and Loman have done fits for the nucleon-nucleon data below 350 MEV using a boundary condition model interaction determined largely by field-theoretic forms. One and two pions, ρ, ω, and η meson exchange adiabatic potentials determine the interaction. Feshbach and Loman applied their potential in the calculation of the deuteron wave functions [4].

J. Stewart has shown experimentally that a correction, ΔG_{en}, due to relativistic modifications of the deuteron wave functions and the nucleon current must be added to Equation

(2-18) [8]. Within the range of momentum transfers studied here this correction is proportional to q^2.

$$\Delta G_{en} \simeq \frac{q^2}{8M_p^2} \qquad (2\text{-}21)$$

III. DATA REDUCTION

A. THE RATIO EXPERIMENT

An experimental cross section may be written in the form

$$\sigma_{exp} = \frac{N_{sc}}{n_t \Delta\Omega} K_S K_B \qquad \text{cm}^2 \text{ ster}^{-1} \qquad (3\text{-}1)$$

where N_{sc} is the number of scattered electrons per microcoulomb of incident electrons, n_t is the number of target atoms per cm^2, $\Delta\Omega$ is the solid angle subtended by the spectrometer, and finally, K_S and K_B are the radiative corrections. The analysis of experimental scattering data is somewhat simplified by a ratio experiment in which several experimental parameters cancel. In general, the scattering data of the interaction under study is normalized to the data of a second interaction for which absolute results are well documented. In these measurements, the e-d scattering data was normalized to e-p scattering data taken in experiments under similar conditions. A ratio of experimental cross sections for deuterium and hydrogen is obtained.

$$\frac{\sigma^d_{exp}}{\sigma^p_{exp}} = \frac{N^d_{sc}}{N^p_{sc}} \cdot \frac{n^p_t}{n^d_t} \cdot \frac{K^d_S}{K^p_S} \cdot \frac{K^d_B}{K^p_B} . \qquad (3\text{-}2)$$

The ratio of the experimental cross section to that predicted for a point nucleon (Mott cross section) yields the experimental form factor, G^2. If appropriate magnetic corrections are applied to the G^2, the charge form factor, G_e^2, is obtained.

$$\frac{G_{ed}^2}{G_{ep}^2} = \frac{N_{sc}^d}{N_{sc}^p} \cdot \frac{n_t^p}{n_t^d} \cdot \frac{\sigma_{Mott}^p}{\sigma_{Mott}^d} \cdot \frac{K_M^d}{K_M^p} \cdot \frac{K_S^d}{K_S^p} \cdot \frac{K_B^d}{K_B^p} . \qquad (3\text{-}3)$$

When variations in the incident energy and momentum transfer between the deuteron and proton analysis are taken into account Equation (3-3) becomes

$$\frac{G_{ed}^2}{G_{ep}^2} = \frac{N_{sc}^d}{N_{sc}^p} \cdot \frac{n_t^p}{n_t^d} \cdot \frac{\sigma_{Mott}^p}{\sigma_{Mott}^d} \cdot \frac{K_M^d}{K_M^p} \cdot \frac{K_S^d}{K_S^p} \cdot \frac{K_B^d}{K_B^p} \cdot \frac{G_{ep}^2(q_p^2)}{G_{ep}^2(q_d^2)} . \qquad (3\text{-}4)$$

Now consider this experimental ratio term by term. First, the ratio of the number of scattered electrons is given by

$$\frac{N_{sc}^d}{N_{sc}^p} = \frac{A_d}{A_p} \cdot \frac{E_p}{E_d} \qquad (3\text{-}5)$$

where A_p and A_d are the areas under the proton and deuteron scattering peaks respectively. If the scattering peaks are plotted as counts per microcoulomb versus energy, then the areas have units of counts-MEV per microcoulomb. A simple ratio of these areas is not sufficient, however, since the spectrometer resolution varies with energy. Hence, a correction for the differing resolution at the proton and deuteron scattering peaks is required. The correction is inversely proportional to energy and therefore, a simple ratio of the proton to deuteron scattering peak energies is a sufficient correction. E_p and E_d are the proton and deuteron peak energies respectively.

The ratio of the number of target atoms n_t^p/n_t^d is composed basically of the gas densities calculated with the appropriate virial coefficients for pressures of approximately 150.0 PSI and temperatures in the liquid nitrogen range. Also included in the ratio is a conversion from density to number of nucleons per cm^2.

$$\frac{n_t^p}{n_t^d} = \frac{\rho_p}{\rho_d} (1.9985). \tag{3-6}$$

σ^p_{Mott} and σ^d_{Mott} are the theoretical cross sections for a point proton and deuteron respectively as given in Equation (2-1).

$$\left(\frac{d\sigma}{d\Omega}\right)_{Mott} = \left(\frac{e^2}{2E_i}\right) \frac{\cos^2 \theta/2}{\sin^4 \theta/2} \left(1 + \frac{2E_i}{M} \sin^2 \theta/2\right)^{-1}$$

where M is the appropriate rest mass for the proton or deuteron.

The magnetic correction terms were derived in the previous chapter.

$$K_M^d = \frac{1}{(1 + C_d)} \tag{3-7}$$

where C_d is given by Equation (2-15) and

$$K_M^p = \frac{(1 + \tau)}{(1 + C_p)} \tag{3-8}$$

where C_p is given by Equation (2-7).

The radiative corrections are of two types. The Schwinger correction accounts for the emission and reabsorption of virtual

photons in the field of the scattering nucleus, nuclear bremsstrahlung, as well as the emission of soft photons of energy less than a specified cutoff energy. The latest and most accurate version of the Schwinger correction is given by Tsai [10]. This expression will later be referred to as Form I.

$$K_S = e^{\delta_S} \tag{3-9}$$

where

$$\begin{aligned}
\delta_S = \frac{\alpha}{\pi}\Bigg\{ & \frac{28}{9} - \frac{13}{6}\ln\left(\frac{q^2}{m^2}\right) + \left(\ln\frac{q^2}{m^2} - 1 + 2Z\ln\xi\right)\cdot \\
& \left(2\ln\frac{E_i}{\Delta E} - 3\ln\xi\right) - \Phi\left(\frac{E_3-E_i}{E_3}\right) - Z^2\ln\frac{E_4}{M} + Z^2\ln\frac{M}{\xi\Delta E}\cdot \\
& \left\{\frac{1}{\beta_4}\ln\frac{1+\beta_4}{1-\beta_4}\ln\frac{E_4+M}{2M} - \Phi\left[-\left(\frac{E_4-M}{E_4+M}\right)^{1/2}\left(\frac{1+\beta_4}{1-\beta_4}\right)^{1/2}\right]\right\} \\
& + Z\Bigg[\Phi\left(-\frac{M-E_3}{E_i}\right) - \Phi\left(\frac{M(M-E_3)}{2E_3E_4-ME_i}\right) + \Phi\left(\frac{2E_3(M-E_3)}{2E_3E_4-ME_i}\right) \\
& + \ln\left|\frac{2E_3E_4-ME_i}{E_i(M-2E_3)}\right|\ln\left(\frac{M}{2E_3}\right)\Bigg] - Z\Bigg[\Phi\left(-\frac{E_4-E_3}{E_3}\right) - \Phi\left(\frac{M(E_4-E_3)}{2E_iE_3-ME_3}\right) \\
& + \Phi\left(\frac{2E_i(E_4-E_3)}{2E_iE_4-ME_3}\right) + \left|\ln\frac{2E_iE_4-ME_3}{E_3(M-2E_i)}\right|\ln\left(\frac{M}{2E_i}\right)\Bigg] - Z\Bigg[\Phi\left(-\frac{M-E_i}{E_i}\right) \\
& - \Phi\left(\frac{M-E_i}{E_i}\right) + \Phi\left(\frac{2(M-E_i)}{M}\right) + \ln\left|\frac{M}{2E_i-M}\right|\ln\left(\frac{M}{2E_i}\right)\Bigg] + Z\Bigg[\Phi\left(-\frac{M-E_3}{E_3}\right) \\
& - \Phi\left(\frac{M-E_3}{E_3}\right) + \Phi\left(\frac{2(M-E_3)}{M}\right) + \ln\left|\frac{M}{2E_3-M}\right|\ln\left(\frac{M}{2E_3}\right)\Bigg] - \frac{\alpha}{\pi}\Bigg(-\zeta\left(\frac{E_i-E_3}{E_3}\right) \\
& + \frac{Z^2}{\beta_4}\left\{\Phi\left[\left(\frac{E_4-M}{E_4+M}\right)^{1/2}\left(\frac{1-\beta_4}{1+\beta_4}\right)^{1/2}\right] - \Phi\left[\left(\frac{E_4-M}{E_4+M}\right)^{1/2}\right] + \Phi\left[-\left(\frac{E_4-M}{E_4+M}\right)^{1/2}\right]\right\}\Bigg)\Bigg\}.
\end{aligned} \tag{3-10}$$

Here E_i is the incident electron energy, E_3 is the energy of the elastic peak (most probable energy of the scattered electron spectrum), $E_4 = E_i + M - E_3$, M is the rest mass of the scattering center, ΔE is the energy interval between the energy of the elastic peak and the lower limit of the scattered electron spectrum, Z is the atomic number of the scattering center, m is the rest mass of the electron, Φ is a Spence function, α is the fine structure constant, and $\beta_4 = (E_4^2 - M^2)^{\frac{1}{2}}/E_4$. Tsai also gives a simplier form of the Swinger correction [9]. This expression will later be referred to as Form II.

$$\delta_S = \frac{2\alpha}{\pi}\left\{\left(\frac{1}{2}\ln\frac{E_i}{\xi^2\Delta E} + \frac{1}{2}\ln\frac{E_3}{\Delta E} - \frac{13}{12}\right)\left[\ln\left(\frac{q^2}{m^2}\right) - 1\right] + \frac{17}{36}\right\} \tag{3-11}$$

The Bethe-Heitler correction accounts for the emission of real photons by bremsstrahlung in the field of atomic electrons and in the field of nuclei other than the target nucleus. Tsai evaluated the Bethe-Heitler correction under the assumption that the scattering occurs midway through the target [10]. This expression will be later referred to as Form I.

$$K_B = e^{\delta_B} \tag{3-12}$$

where

$$\delta_B = \left\{\left[b_w T_{iw} + \frac{1}{2}bT\right]\ln\left(\frac{E_i}{\xi^2\Delta E}\right) + \left[b_w T_{fw} + \frac{1}{2}bT\right]\ln\left(\frac{E_3}{\Delta E}\right)\right\} \tag{3-13}$$

Here T_{iw} is the entrance window thickness and T_{fw} is the exit window thickness. Bethe and Ashkin give a simple form

of the above [5]. This expression will later be referred to as Form II.

$$\delta_B = \frac{T\rho}{\chi_0} \frac{1}{\cos\phi \ln 2} \ln \frac{E_i}{\Delta E \xi^{3/2}} \qquad (3\text{-}14)$$

Here T is the target thickness, ϕ is the angle the target makes with the incoming electron, ρ is the target density, and χ_0 is the characteristic radiation length of the target material. For the gas target ϕ is set to zero and T is calculated geometrically as an effective thickness dependent upon the target chamber dimensions, scattering angle, spectrometer entrance port, etc.

The radiative corrections of both forms were calculated for the data considered here. A composite radiative correction, $(K_S^d K_B^d / K_S^p K_B^p)$, for the experimental form factor ratio was then obtained using the corrections of Form I and another using the corrections of Form II. Very little significant difference was found between the two forms when used in calculating the form factor ratio. A summary of these calculations is found in Table I.

Another correction resulting from ionization loss, or Landau straggling has been ignored since the effect is nearly identical for the hydrogen and deuterium targets.

Finally, the correction for variations in incident energy and momentum transfer between the deuteron and proton analysis is given by a ratio of proton form factors at the differing momentum transfers $(G_{ep}^2(q_p^2)/G_{ep}^2(q_d^2))$. Because the results of electron-proton scattering are well documented,

q^2	Uncorr. G_{ed}^2/G_{ep}^2	$K_S^d K_B^d / K_S^p K_B^p$ I	$K_S^d K_B^d / K_S^p K_B^p$ II	G_{ed}^2/G_{ep}^2 I	G_{ed}^2/G_{ep}^2 II
0.0657	0.8565	1.0028	1.0026	0.8589	0.8587
0.0999	0.9122	1.0017	1.0028	0.9137	0.9147
0.1000	0.8507	0.9980	0.9997	0.8490	0.8505
0.1578	0.8266	1.0019	1.0032	0.8281	0.8293
0.1610	0.8619	0.9970	0.9993	0.8593	0.8612
0.1610	0.7777	1.0012	1.0029	0.7786	0.7799
0.2001	0.7848	0.9974	0.9995	0.7828	0.7844
0.3618	0.6384	0.9998	1.0074	0.6383	0.6431
0.3618	0.6581	1.0019	1.0046	0.6594	0.6612
0.3957	0.6270	0.9976	1.0007	0.6256	0.6275
0.4000	0.6490	0.9889	1.0019	0.6483	0.6502
0.5001	0.5783	0.9950	0.9987	0.5754	0.5776
0.5760	0.5347	1.0003	1.0038	0.5349	0.5368

Table I Comparison of Radiative Correction Calculations

I and II refer to the forms of the radiative corrections outlined on pages 18-20.

an absolute value of G_{ep}^2 can be determined. The total proton form factor, G_p^2, is found utilizing a de Vries b' fit determination [2] and then the magnetic correction, K_M^p, found in Equation (3-9), is applied to obtain G_{ep}^2.

Equation (2-18) for the neutron form factor may be written

$$\frac{G_{en}}{G_{ep}} = \frac{1}{F_d}\left[\frac{G_{ed}}{G_{ep}}\right] - 1 \qquad (3\text{-}15)$$

and therefore, the ratio, G_{en}/G_{ep}, is obtained experimentally from G_{ed}/G_{ep} of Equation (3-4). As explained above, an absolute value of G_{ep} is available to extract G_{en} from the ratio.

B. ANALYSIS OF SCATTERING PEAKS

The results of a typical scattering experiment are shown in Figure 1 which plots the scattered electron spectrum (counts per microcoulomb versus energy). The average background, as determined from data at energies above the peak energy, is shown as a constant value. To obtain the total area under the peak a simple 3-point numerical integration technique was used. The area used in calculating N_{sc} is computed by subtracting the background area (average background multiplied by the integration range) from the integration result.

Deuteron and proton scattering data was obtained in two ways. In the first case a target containing both hydrogen and deuterium gas in known quantities was analyzed. A

typical result is shown in Figure 2. A_d is obtained accurately as long as the integration range falls short of the proton peak and the deuteron inelastic tail. Since the proton peak rides on the deuteron inelastic peak, extracting A_p is more involved than outlined above. To remove the deuteron inelastic peak a second scattering experiment was performed under similar conditions. The results of the second experiment with pure deuterium which matches the conditions of the experiment of Figure 2 are shown in Figure 3. The separate pure deuterium target data was scaled to the mixture data according to the area under the elastic deuteron peaks. The scaled inelastic peak together with the background area is subtracted from the proton integration result to obtain A_p. Some difficulty was found in this method. The separation of the proton and deuteron peaks is proportional to the momentum transfer of the measurement. A comparison between data at $q^2 = 0.1610$ and $q^2 = 0.3618$ may be found in Figures 2 and 4. Notice in the data for $q^2 = 0.1610$ that the counts between the peaks do not fall to background. Hence, there is some ambiguity in integrating under the peaks which remains unresolved even with the subtraction if the scaled deuteron inelastic peak. For this and other reasons to be mentioned later the measurements which utilized gas mixtures at low momentum transfers were neglected.

The second method of measurement involves two separate experiments under similar conditions. A pure deuterium gas target is analyzed in one and a pure hydrogen target is analyzed in the other. If the incident energies are adjusted

properly in the two measurements, identical momentum transfer can be achieved and the results can be compared with only minor corrections. The calculations of A_p and A_d follow the same method outlined at the beginning of this section. In this case, however, there is no interference between the peaks and therefore, the areas can be calculated very accurately.

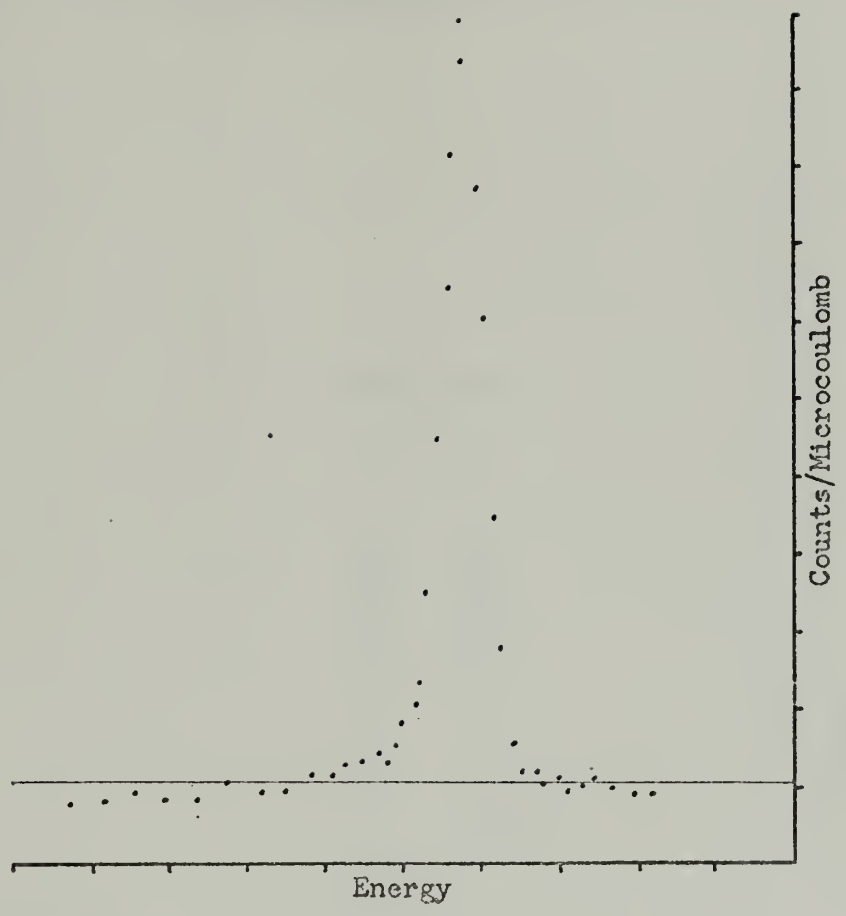

Figure 1 Hydrogen Elastic Peak at 0.1534 F^{-2}

E_i = 56.255 MEV

Theta = 90°

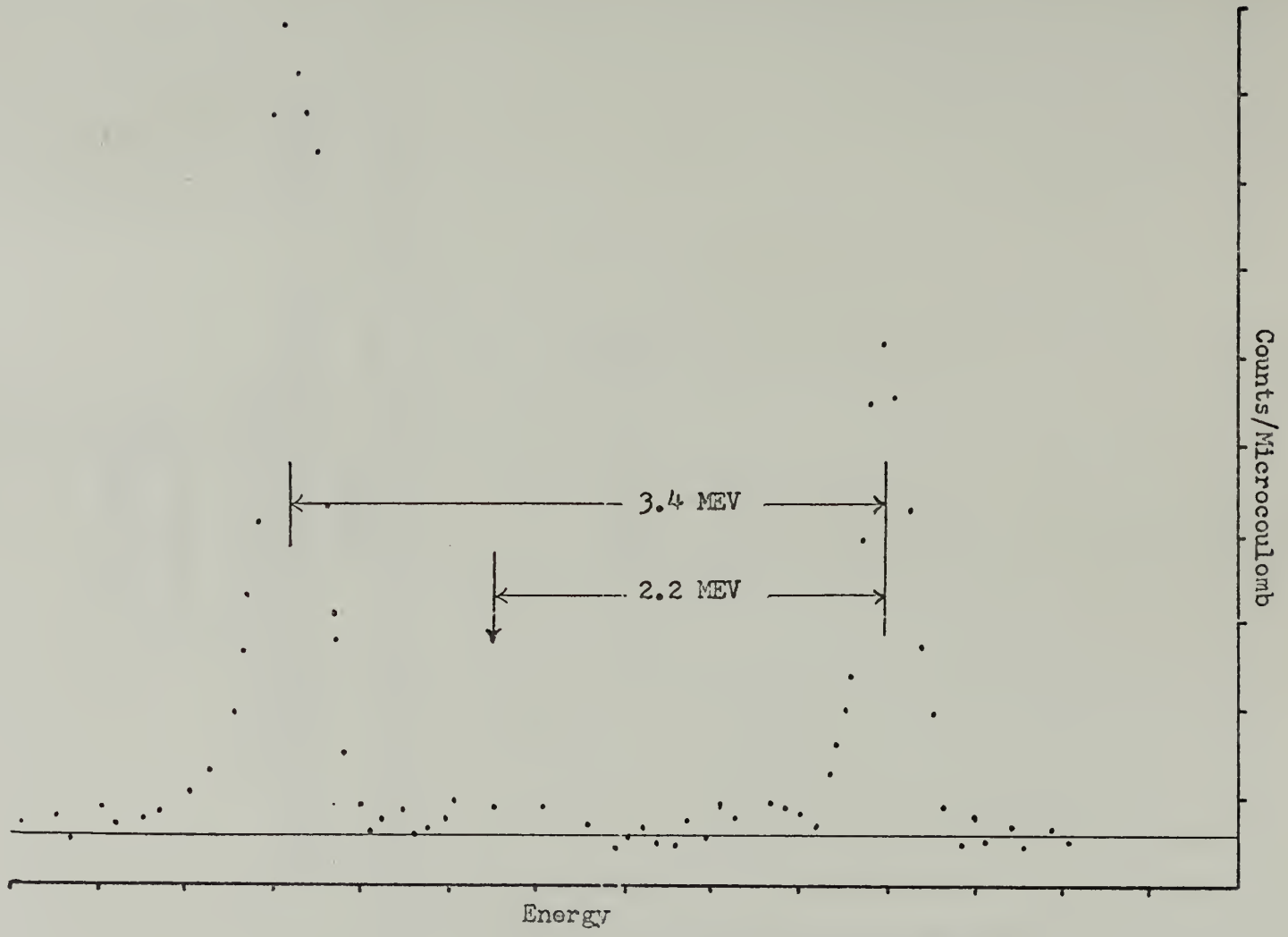

Figure 2 Mixture Experiment at 0.3618 F^{-2}

E_i = 70.424 MEV, q_d^2 = 0.3618 F^{-2}, q_p^2 = 0.3435 F^{-2}, Theta = 120°

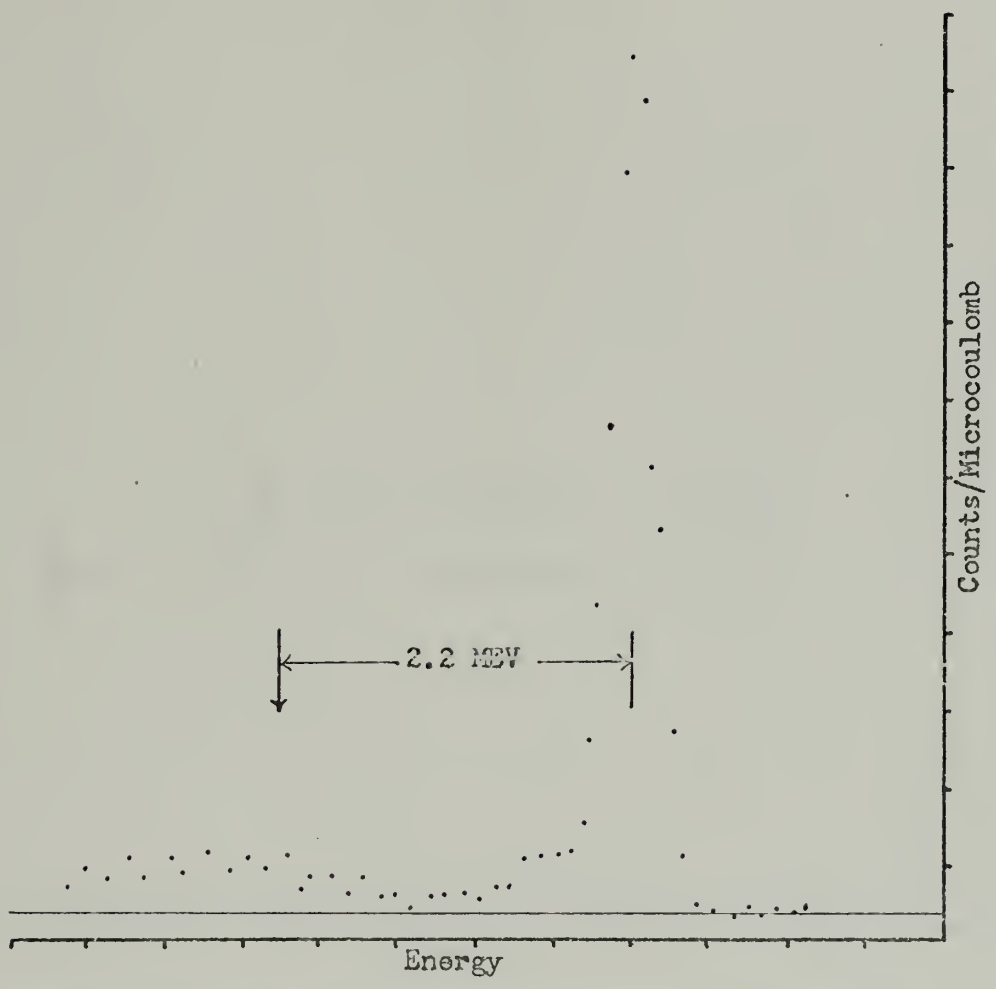

Figure 3 Deuterium Experiment at 0.3618 F^{-2} with Elastic and Inelastic Peaks

E_i = 70.424 MEV

Theta = 120°

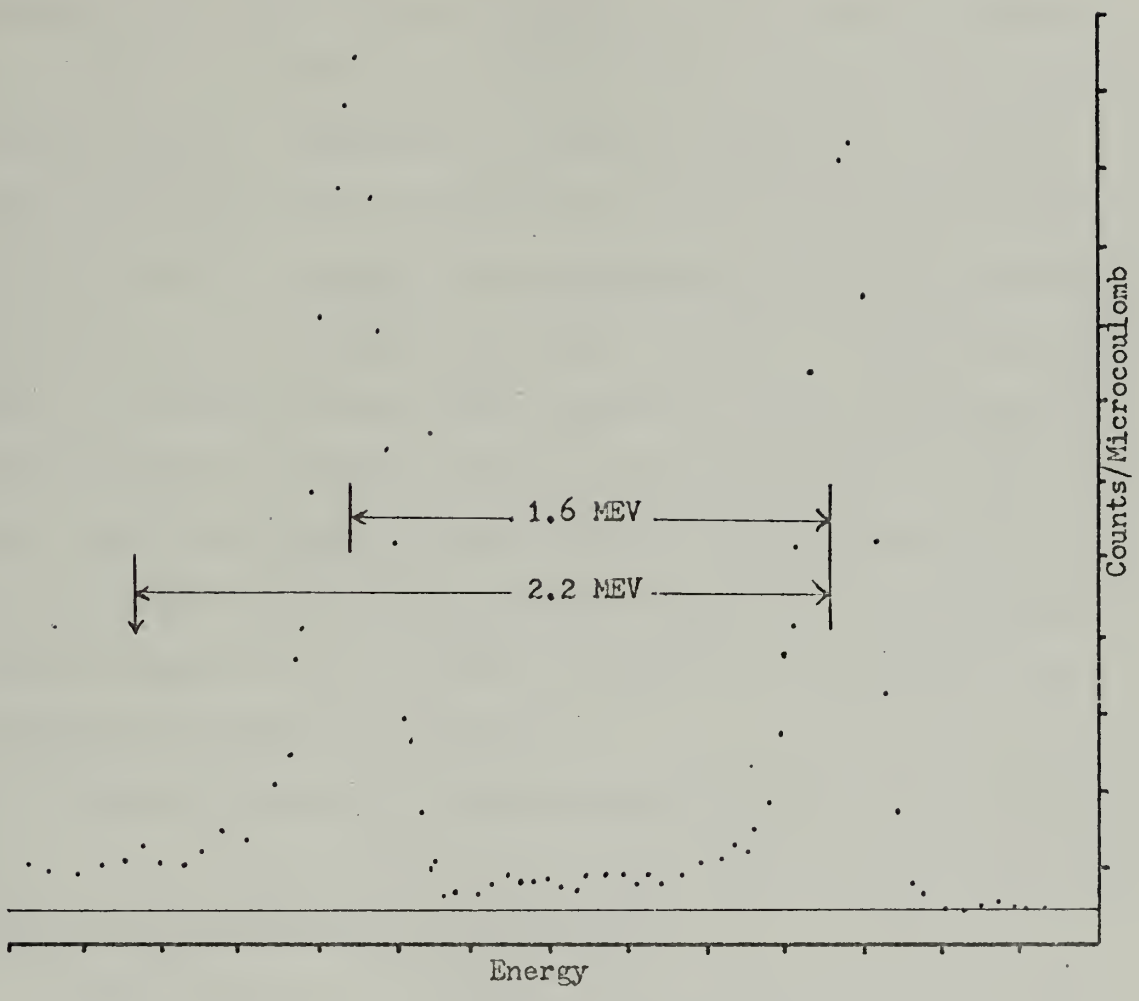

Figure 4 Mixture Experiment at 0.1610 F^{-2}

E_i = 46.561 MEV

q_d^2 = 0.1610 F^{-2}

q_p^2 = 0.1555 F^{-2}

Theta = 120°

IV. RESULTS

Table II gives a summary of the calculations for the charge form factor ratio, G_{ed}^2/G_{ep}^2, to four place accuracy.

Table III lists the values of the charge form factor ratio, G_{ed}/G_{ep}, and gives two least squares fits to the data. The first fit includes all the experimental points. The second fit excludes the measurements noted as mixtures at the lowest momentum transfers. Because of the difficulties in determining the peak areas for these experiments, as mentioned in Section III-B, and due to the fact that they lower the G_{ed}/G_{ep} intercept in a least squares fit considerably from its theoretical value of 1, the experimental points at $q^2 = 0.0657\ F^{-2}$ and $q^2 = 0.1610\ F^{-2}$ are neglected in the final analysis.

Figure 5 shows the experimental points of Table III plotted. In addition, the two least squares fits noted in Table III are shown for comparison.

Table IV gives a summary of the calculations for the neutron charge form factor, G_{en}, with relativistic corrections. The values listed for the deuteron structure factor are computed utilizing Feshbach-Loman wave functions. The values of G_{ep} are calculated utilizing de Vries b' fit. A least squares fit to a n-e slope, $dG_{en}/d(q^2)$, was computed and the results are listed. In addition, a weighted average of the G_{en} values was determined. It should be noted, on the basis of the errors in the least squares fit compared

to the errors in the weighted average, that the experimental points are best suited to a constant value fit of approximately zero.

Figure 6 shows the experimental points of Table IV plotted. The line which is drawn with the greatest slope represents the accepted value for the neutron-electron interaction slope.

$$dG_{en}/d(q^2) = 0.0193 + \text{or} - 0.004.$$

The line drawn with the smaller slope is that of the least squares fit noted in Table IV. The constant value line shown is that of the weighted average noted in Table IV.

In summary, these experiments in electron-deuteron scattering have not shown agreement with the results of previous experiments. These measurements with gas targets show little or no slope in the n-e interaction curve for very low momentum transfers. To date no explanation of these results has been found.

q^2	Theta	$\frac{A_d E_p}{A_p E_d}$	$\frac{\sigma^p_{Mott}}{\sigma^d_{Mott}}$	n^p_t/n^d_t	K^d_M/K^p_M	$\frac{K^d_S K^d_B}{K^p_S K^p_B}$	$\frac{G^2_{ep}(q^2_p)}{G^2_{ep}(q^2_d)}$	G^2_{ed}/G^2_{ep}	% Error	Notes
0.0657	60	0.9060	0.9868	0.9503	1.0080	1.0026	1.0002	0.8587	0.83	Mixture
0.0999	120	0.9186	0.9442	0.9970	1.0550	1.0028	0.9999	0.9147	0.91	-
0.1000	90	0.8741	0.9542	0.9970	1.0231	0.9997	1.0000	0.8505	0.88	-
0.1578	90	0.8234	0.9717	0.9970	1.0351	1.0032	1.0010	0.8293	0.85	-
0.1610	90	0.9004	0.9715	0.9502	1.0358	0.9993	1.0010	0.8612	1.26	Mixture
0.1610	120	0.7803	0.9654	0.9502	1.0849	1.0029	1.0013	0.7799	1.11	Mixture
0.2001	90	0.8042	0.9360	0.9970	1.0437	0.9995	1.0000	0.7844	0.92	-
0.3618	90	0.6477	0.9581	0.9503	1.0788	1.0074	1.0035	0.6431	1.22	Mixture
0.3618	120	0.6125	0.9495	0.9503	1.1857	1.0046	1.0043	0.6612	1.26	Mixture
0.3957	90	0.6031	0.9563	0.9970	1.0860	1.0007	1.0040	0.6275	0.81	-
0.4000	120	0.6002	0.8914	0.9970	1.2166	1.0019	1.0000	0.6502	0.92	-
0.5001	120	0.5195	0.8796	0.9970	1.2694	0.9987	0.9999	0.5776	0.83	-
0.5760	120	0.4706	0.8705	0.9969	1.3095	1.0038	0.9998	0.5368	0.91	-

Table II A Summary of Calculations for G^2_{ed}/G^2_{ep}

q^2	G_{ed}/G_{ep}	+ or -	Notes
0.0657	0.9267	0.0077	Mixture
0.0999	0.9564	0.0087	-
0.1000	0.9222	0.0081	-
0.1578	0.9106	0.0077	-
0.1610	0.8831	0.0098	Mixture
0.1610	0.9280	0.0117	Mixture
0.2001	0.8856	0.0081	-
0.3618	0.8131	0.0102	Mixture
0.3618	0.8019	0.0098	Mixture
0.3957	0.7921	0.0064	-
0.4000	0.8063	0.0074	-
0.5001	0.7600	0.0063	-
0.5760	0.7326	0.0067	-

Least Squares Fits to $G_{ed}/G_{ep} = A + B(q^2) + C(q^2)^2$

1. Utilizing all experimental points:

   A = 0.9757 + or - 0.0085
   B = - 0.4722 + or - 0.0340
   C = 0.0775 + or - 0.0090

2. Utilizing experimental points other than those noted as mixtures at momentum transfers less than 0.2 inverse Fermis squared:

   A = 0.9976 + or - 0.0110
   B = - 0.6088 + or - 0.0504
   C = 0.2621 + or - 0.0336

Table III Least Squares Fits for G_{ed}/G_{ep}

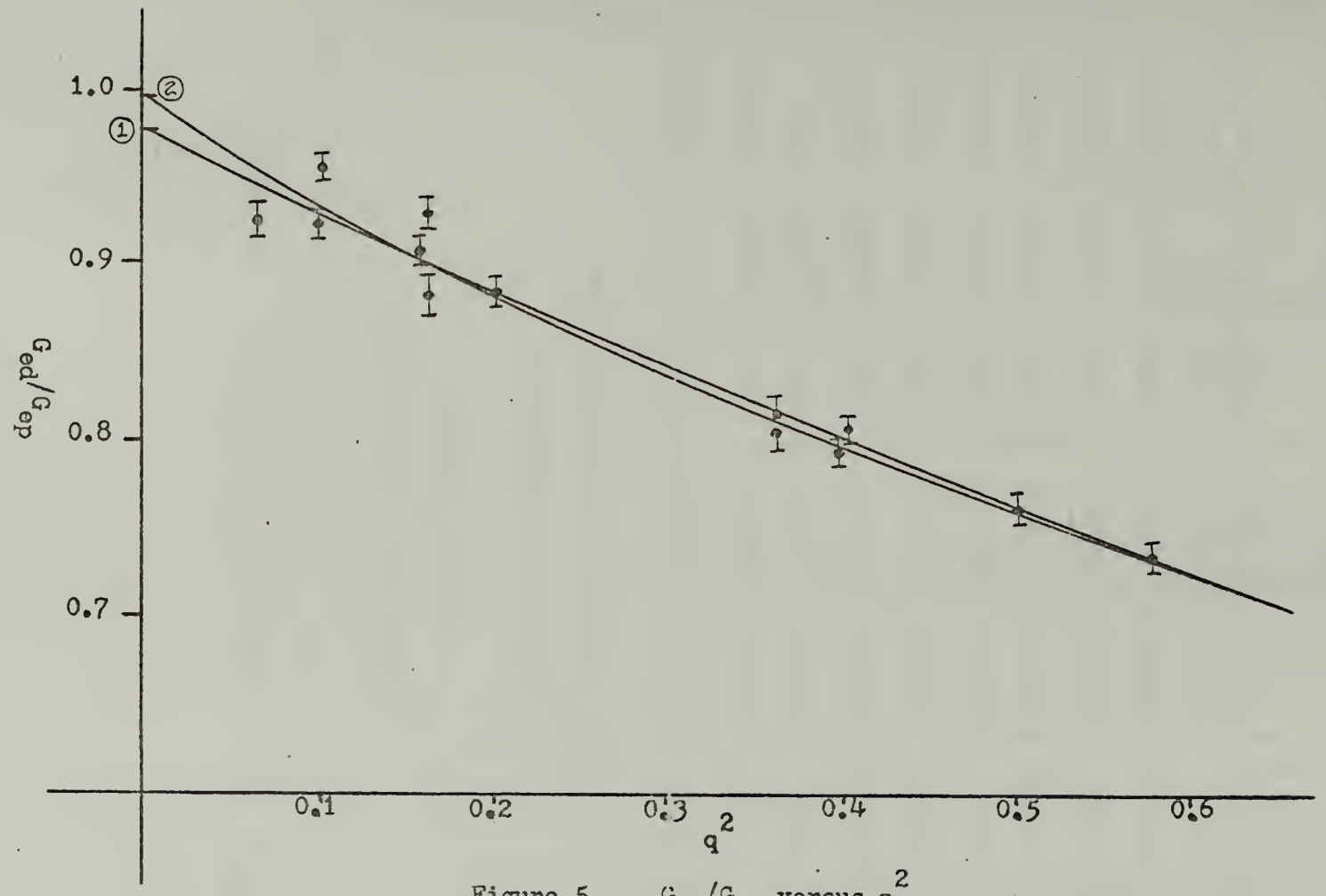

Figure 5 G_{ed}/G_{ep} versus q^2

1. Least squares fit utilizing all experimental points
2. Least squares fit utilizing experimental points other than those noted as mixtures at momentum transfers less than 0.2 inverse Fermis squared

q^2	F_d	G_{ep}	G_{en}	ΔG_{en}	$G_{en}+\Delta G_{en}$	+ or -
0.0999	0.9398	0.9881	0.0175	0.00055	0.0180	0.0093
0.1000	0.9398	0.9881	-0.0185	0.00055	-0.0180	0.0086
0.1578	0.9081	0.9815	0.0027	0.00087	0.0036	0.0085
0.2001	0.8867	0.9765	-0.0012	0.00110	-0.0001	0.0092
0.3618	0.8134	0.9584	-0.0136	0.00200	-0.0116	0.0120
0.3618	0.8134	0.9584	-0.0004	0.00200	0.0016	0.0126
0.3857	0.7986	0.9545	-0.0078	0.00218	-0.0056	0.0080
0.4000	0.7976	0.9540	0.0104	0.00221	0.0126	0.0093
0.5001	0.7596	0.9431	0.0005	0.00276	0.0033	0.0083
0.5760	0.7330	0.9350	-0.0005	0.00318	0.0027	0.0091

Least Squares Fit to $G_{en}+\Delta G_{en} = B(q^2)$

$B = 0.0032$ + or - 0.0031

Weighted Average

$WA = 0.0019$ + or - 0.0006

Table IV A Summary of Calculations for $G_{en} + \Delta G_{en}$

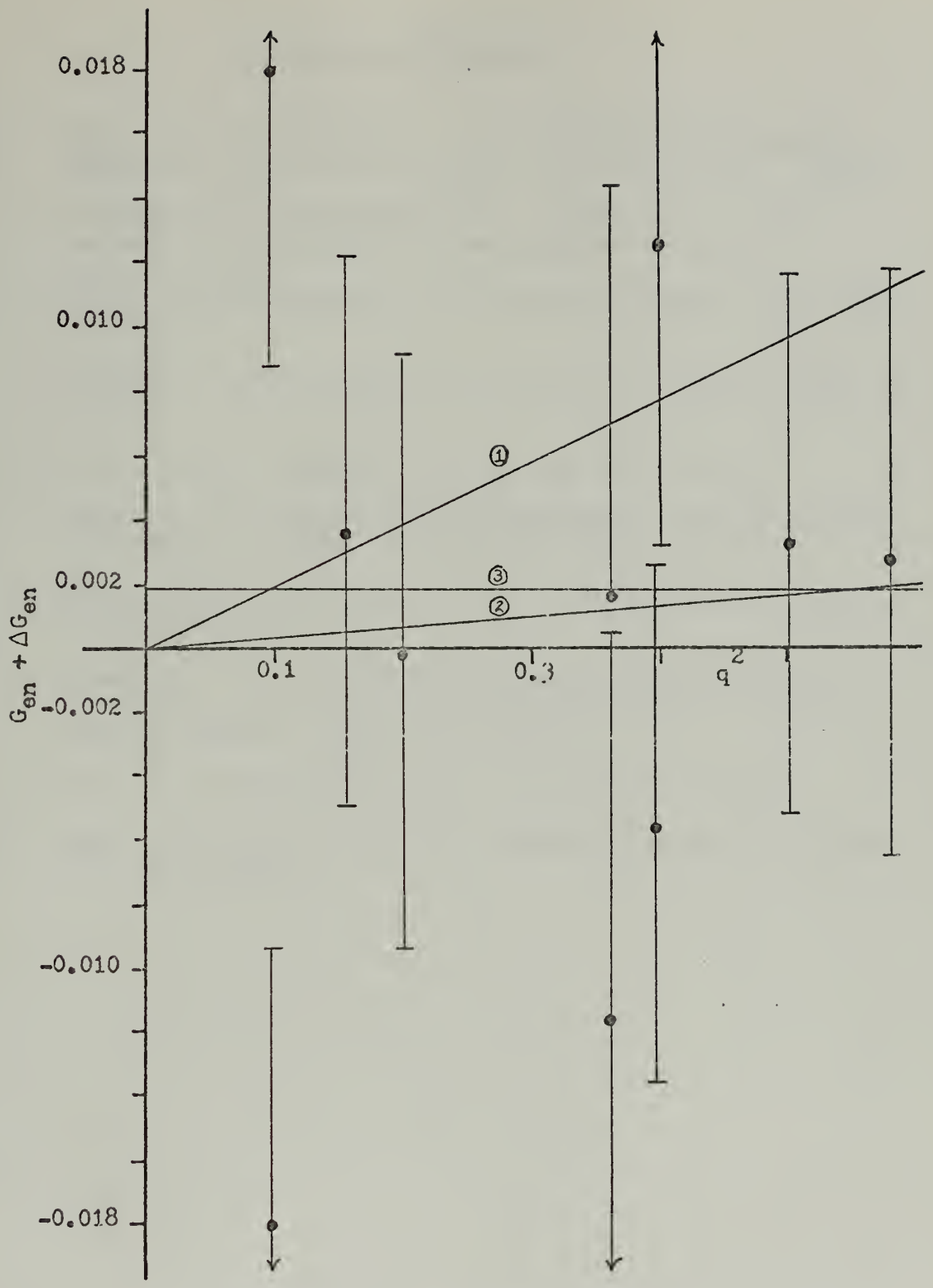

Figure 5 $G_{en} + \Delta G_{en}$ versus q^2

1. N-e interaction slope
2. Least squares fit of experimental points to a slope
3. Weighted average of experimental points

LIST OF REFERENCES

1. Bethe, H. A. and Ashkin, J., Experimental Nuclear Physics, John Wiley and Sons, Inc., New York (1953).

2. de Vries, C., Hofstadter, R., Johansson, A. and Herman, R., Physics Review, 134, B848 (1964).

3. Fermi, E. and Marshall, L., Physics Review, 72, 1139 (1947).

4. Feshbach, H. and Loman, E., Annals of Physics, 48, 94 (1968).

5. Foldy, L. L., Physics Review, 87, 693 (1952).

6. Hughes, D. J., Pile Neutron Research, Addison Wesley Publishing Company, Cambridge, Mass. (1953).

7. Krohn, V. E. and Ringo, G. R., Physics Review, 148, 1303 (1966).

8. Stewart, J. W., Naval Postgraduate School Thesis, June 1970. Final results are published in Physics Review Letters, 25, 1774 (1970).

9. Tsai, Y. S., Physics Review, 122, 1898 (1961).

10. Tsai, Y. S. and Mo, L. W., Review of Modern Physics, 41, 205 (1969).

INITIAL DISTRIBUTION LIST

		No. Copies
1.	Defense Documentation Center Cameron Station Alexandria, Virginia 22314	2
2.	Library, Code 0212 Naval Postgraduate School Monterey, California 93940	2
3.	Professor F. R. Buskirk Department of Physics Naval Postgraduate School Monterey, California 93940	10
4.	ENS. Thomas W. Mader, USN 718 Braidwood Lane Orlando, Florida 32803	1

UNCLASSIFIED

Security Classification

DOCUMENT CONTROL DATA - R & D

(Security classification of title, body of abstract and indexing annotation must be entered when the overall report is classified)

1. ORIGINATING ACTIVITY (Corporate author)	2a. REPORT SECURITY CLASSIFICATION
Naval Postgraduate School Monterey, California 93940	UNCLASSIFIED
	2b. GROUP

3. REPORT TITLE

NEUTRON FORM FACTORS FROM ELASTIC ELECTRON-DEUTERON SCATTERING

4. DESCRIPTIVE NOTES (Type of report and, inclusive dates)

Master's Thesis, June 1971

5. AUTHOR(S) (First name, middle initial, last name)

Thomas Walter Mader

6. REPORT DATE	7a. TOTAL NO. OF PAGES	7b. NO. OF REFS
June 1971	39	10

8a. CONTRACT OR GRANT NO.	9a. ORIGINATOR'S REPORT NUMBER(S)
b. PROJECT NO.	
c.	9b. OTHER REPORT NO(S) (Any other numbers that may be assigned this report)
d.	

10. DISTRIBUTION STATEMENT

Approved for public release; distribution unlimited.

11. SUPPLEMENTARY NOTES	12. SPONSORING MILITARY ACTIVITY
	Naval Postgraduate School Monterey, California 93940

13. ABSTRACT

Utilizing a gas target in electron-deuteron and electron-proton scattering, measurements of the ratio of the deuteron to proton form factor, G_{ed}/G_{ep}, were made within a precision of 0.8 to 1.3 percent for the range of momentum transfers, q^2, from 0.05 to 0.60 inverse Fermis squared and for scattering angles between 60 and 120 degrees. From G_{ed}/G_{ep} the neutron to proton form factor ratio, G_{en}/G_{ep}, was extracted utilizing the deuteron structure factor, as calculated from the Feshbach-Loman wave functions, and relativistic corrections. The values of G_{en}/G_{ep} found failed to support previous measurements which agreed with the thermal neutron-electron interaction slope.

DD FORM 1 NOV 65 1473 (PAGE 1)

S/N 0101-807-6811

UNCLASSIFIED

Security Classification

A-31408

KEY WORDS	LINK A		LINK B		LINK C	
	ROLE	WT	ROLE	WT	ROLE	WT
Neutron Form Factors						

Thesis
M27485 Mader
c.1
128579
Neutron form factors
from elastic electron-
deuteron scattering.